Notch-based speed trajectory optimisation for high-speed railway automatic train operation

Minling Feng[1,2], Chaoxian Wu[1,2], Shaofeng Lu[1,2] and Yihui Wang[2]

Abstract

Automatic train operation (ATO) systems are fast becoming one of the key components of the intelligent high-speed railway (HSR). Designing an effective optimal speed trajectory for ATO is critical to guide the high-speed train (HST) to operate with high service quality in a more energy-efficient way. In many advanced HSR systems, the traction/braking systems would provide multiple notches to satisfy the traction/braking demands. This paper modelled the applied force as a controlled variable based on the selection of notch to realise a notch-based train speed trajectory optimisation model to be solved by mixed integer linear programming (MILP). A notch selection model with flexible vertical relaxation was proposed to allow the traction/braking efforts to change dynamically along with the selected notch by introducing a series of binary variables. Two case studies were proposed in this paper where Case study 1 was conducted to investigate the impact of the dynamic notch selection on train operations, and the optimal result indicates that the applied force can be flexibly adjusted corresponding to different notches following a similar operation sequence determined by optimal train control theory. Moreover, in addition to the maximum traction/braking notches and coasting, medium notches with appropriate vertical relaxation would be applied in accordance with the specific traction/braking demands to make the model feasible. In Case study 2, a comprehensive numerical example with the parameters of CRH380AL HST demonstrates the robustness of the model to deal with the varying speed limit and gradient in a real-world scenario. The notch-based model is able to obtain a more realistic optimal strategy containing dynamic notch selection and speed trajectory with an increase (1.622%) in energy consumption by comparing the results of the proposed model and the non-notch model.

Keywords

Notch-based model, mixed integer linear programming, automatic train operation, high-speed railway, train speed optimisation

Introduction

With the rapid development of automatic train operation (ATO), railway systems advance with a deeper degree of automation, higher energy efficiency, and better operation service.[1] The successful experimental field test of ATO equipped in Beijing-Shenyang high-speed railway (HSR) in 2018 marks a significant breakthrough in the application of intelligent HSR.[2] In spite of this, real-world implementations of ATO are still limited to the urban rail systems, and a wider application of ATO in HSRs needs more studies and experimental verification.[3]

Amongst different key technologies for intelligent HSR, designing an efficient optimal speed-distance reference trajectory plays a critical role in ATO system.[4] The relationship between the optimal speed trajectory and the on-board ATO equipped on the high-speed train (HST) is shown in Figure 1. By collecting required static and dynamic information of HSR, an optimisation model is constructed and

[1]Shien-Ming Wu School of Intelligent Engineering, South China University of Technology, Guangzhou, China
[2]State Key Lab of Rail Traffic Control and Safety, Beijing Jiaotong University, Beijing, China

Corresponding authors:
Shaofeng Lu, Shien-Ming Wu School of Intelligent Engineering, South China University of Technology, Guangzhou 511442, China.
Email: lushaofeng@scut.edu.cn
Yihui Wang, State Key Lab of Rail Traffic Control and Safety, Beijing Jiaotong University, Beijing 100044, China.
Email: yihui.wang@bjtu.edu.cn

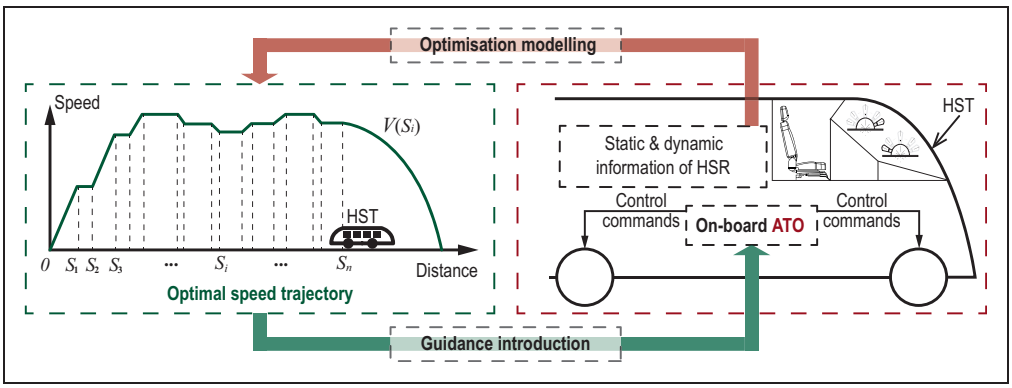

Figure 1. The schematic diagram of the relationship between the optimal speed trajectory and the on-board automatic train operation (ATO). $V(S_i)$ represents the optimal speed trajectory offered to the on-board ATO to ensure a safe and efficient train operation for HST.

relevant algorithms are designed to obtain the optimal train speed trajectory. By doing so, the on-board ATO outputs a series of control commands to the traction transmission system under the guidance, to guide the HST to carry out safe, energy-efficient and punctual operation under various practical constraints. Consequently, it can be concluded that the speed trajectory is fundamental to realise the function of ATO.

Since the 1960s, optimisation of train speed trajectory has been studied extensively in the field of rail transportation. In previous studies, the Pontryagin's maximum principle (PMP) has been widely applied as an indirect method to derive optimal regimes consisting of full traction, cruising, coasting and full braking by using co-state variable.[5–8] Apart from the indirect method, some direct method such as mathematical programming relying on numerical iteration is also utilised extensively with the rapid development of computer technology. Lai et al. utilised dynamic programming and mixed integer linear programming (MILP) to formulate the energy-efficient speed trajectory problem of the medium-speed maglev system considering the impact of auxiliary stopping areas and non-linear resistance.[9] Goverde et al. applied a computational framework that connects pseudospectral methods with the minimum-time train control (MTTC) problem and energy-efficient train control (EETC) problem, aiming at improving the flexibility and accuracy of calculation.[10] Trivella et al. focused on the impact of wind speed and direction on the train resistance which affects the energy consumption and obtained the "wind-aware" train speed trajectory by adopting dynamic programming.[11]

With the rapid development of HSR, the research on the EETC issue for HST has gradually attracted attention from academia and industry in recent years. Different from the urban rail transit, HSR faces challenges from long-distance transportation, high-speed operation and complexity of railway network, etc.[12] To achieve a more intelligent and efficient ATO system of HSRs, it is necessary to establish an optimisation model that can accurately simulate the actual characteristics of the HSR.[13] For this reason, many scholars put forward different algorithms to deal with the speed trajectory schedule problem aiming to consider the above-mentioned HSR operation characteristics.

In order to deal with the uncertainties that may occur on the long-distance HSR lines in real time, many online algorithms have been studied, among which model predictive control (MPC) and rolling horizon optimisation are the most widely used. Apart from the traditional global optimisation, MPC conducts optimisation calculation in each sampling horizon, which can timely deal with various complex situations during the control process. Zhou et al. proposed a MPC model to predict the potential conflicts, keeping the operation safety and robustness while maintaining energy-efficient operation for HST.[14] Moreover, the operation synergies for overtaking and overtaken trains toward junctions in a railway network were formulated after conflict prediction and resolution. Zhong et al. formulated the online speed trajectory optimisation problem based on MPC.[15] By combining both the energy-efficient and time-optimal train control strategies at each control step, the optimisation problem was solved by the pseudospectral method. Besides, a delay recovery process was designed to reschedule the train operation process in the off-on-line model. He et al. proposed a shrinking horizon MPC algorithm, which fully considered the real-time traffic information and solved the energy-efficient HST speed trajectory by applied Radau Pseudo-spectral method.[16] Yan et al. proposed a moving horizon optimisation approach which is based on the immune differential evolutionary algorithm to construct the dynamic train speed trajectory considering the uncertain resistance coefficients, temporary speed restrictions and time delay.[17] Further, a weights allocation was introduced to adjust the energy-saving effect and punctuality.

In the above review, traction/braking characteristics are generally regarded as continuous without considering its intrinsic notch-induced discrete traction/braking characteristics. In many advanced HSR

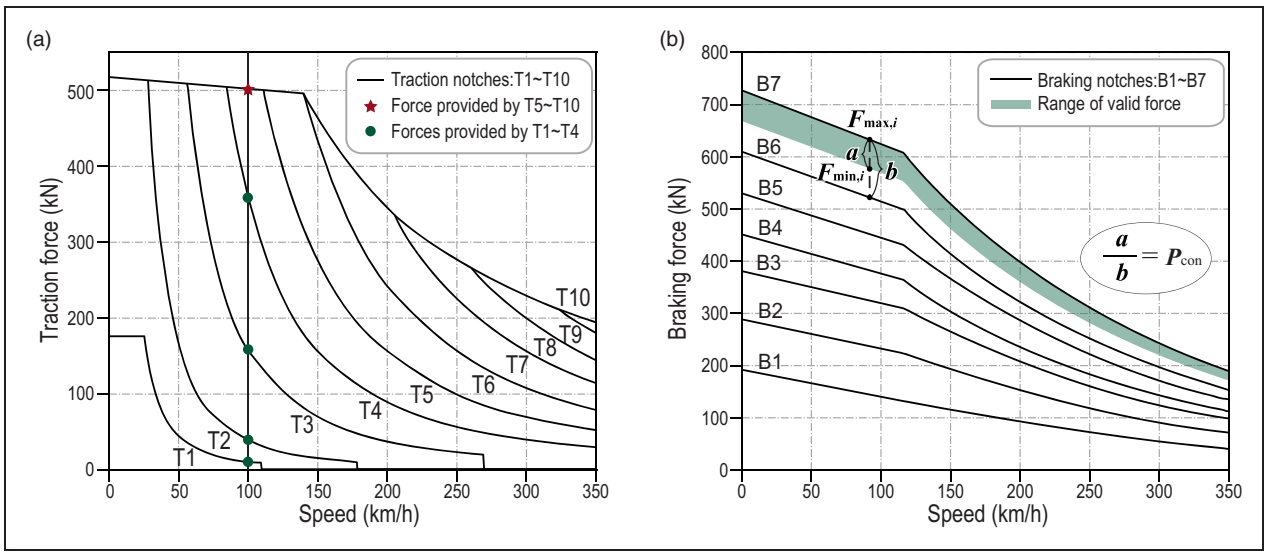

Figure 2. Traction/braking characteristics of CRH380A(L) railway vehicles. (a) it demonstrates 10 traction characteristic curves of HST and shows 5 possible traction forces when the speed of the train is 100 km/h which are corresponding to different notch characteristics. (b) it illustrates 7 braking characteristic curves of HST, and visualises the vertical relaxation for the case when the notch is selected at B7. The valid force range a is determined by a distance b between the braking characteristic curves defined by B7 and B6 and the control factor P_{con}.

systems, the traction/braking system would provide multiple notches to satisfy the traction/braking demands. For example, China CRH series HSTs have 10 traction notches and 7 braking notches,[18] as shown in Figure 2. With the multiple notches for a single train, various choice of notches will lead to different applied forces from the traction/braking system. Accordingly, it is necessary to consider the impact of the dynamic change of the notches while planning the speed trajectory for HSTs. Based on the above review, it is found that though notch information has been regarded as key engineering characteristic for HSTs, the impact of notch selection on train operations still worth further study.

Based on the multi-notch characteristics, some studies were carried out in the field of optimal control of heavy haul freight train whose electric locomotives are also equipped with multiple discrete notches to provide high power for the operations. Zhang et al. formulated the operation control problem with a consideration of energy consumption, velocity tracking, and operation safety for the heavy-haul freight trains, and the problem is solved by a MPC model. The traction/braking efforts characteristics determined by the multiple notches were approximated as cubic functions of $1/v$.[19] Tang et al. processed the control notches as actions which were approximated as a nonlinear function. By introducing a novel Double-Switch Q-network improved from the traditional Q-network, the optimal control of heavy-haul freight train formulated as a standard reinforcement learning problem was realised with three objectives, consisting of velocity, energy consumption and coupler force.[20]

Regarding the treatment of multi-notch characteristics of HST, studies were dedicated to the speed tracking process rather than the train speed trajectory optimisation.[21,22] In some speed trajectory optimisation research, the multi-notch characteristics of HST were simply considered. Li et al. introduced step functions to address the switch problem of notches, and the optimal control problem was transformed into an optimisation problem to calculate a vector containing comprehensive notch information by applying Genetic Algorithm (GA).[23] Zhang et al. proposed a receding horizon-particle swarm optimization to regulate the optimal speed trajectory offline and adjusted the target speed trajectory dynamically under a temporary speed restriction where a multi-notch model was introduced.[24] However, in their notch selection models, each notch is simplified to be a ratio of the characteristic curve determined by the maximum notch, but this does not reflect the realistic notch characteristics in practice as shown in Figure 2.

In this paper, a MILP model was put forward to schedule the optimal speed trajectory with regard to the energy-efficient operation for HSR under various practical constraints, such as punctuality, varying speed limit and varying gradient, etc. Moreover, a novel notch selection model was proposed to simulate the dynamic applied force changing along with the speed with a consideration of the variable notches by introducing a series of binary variables to determine the corresponding notches. Furthermore, a vertical relaxation mechanism was developed to ensure a feasible and efficient solution wherein a relaxation factor controls the valid range of the applied force. A piecewise linearisation (PWL) modelling technique was applied to deal with the non-linear variables which is of benefit to decrease the model complexity and improve the calculation efficiency. Finally,

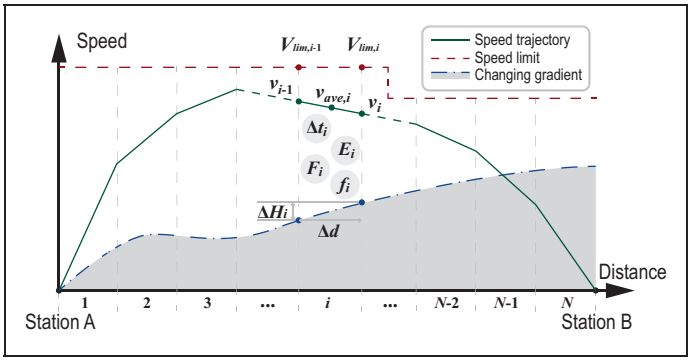

Figure 3. Schematic of an optimal speed trajectory connected by a series of discretised segments with index number from 1 to N.

numerical examples adopting the data of China CRH380A(L) HST were conducted to illustrate the effectiveness of the proposed model.

The main contributions of this paper are as follows.

(i) Different from previous studies, this paper presented a notch-based speed trajectory optimisation model, which is able to optimise both notch strategy and speed trajectory.
(ii) An innovative vertical relaxation technique was proposed in solving the model to address the infeasibility issue due to the discrete characteristic of the model and finite notches. This technique allows a close approximation of notch-based operation and avoid the situation where infeasible solution is resulted.
(iii) To realise the efficient notch selection, a series of binary variables corresponding to each traction/braking characteristic were introduced, allowing a dynamic variation of the applied force according to the changing speed and notch numbers.

Model formulation

In this paper, the whole journey of HST was discretised based on distance. By conducting modelling based on MILP, every discrete segment is connected into a complete optimal speed trajectory while maintaining a reasonable balance between high computational efficiency and calculation accuracy by selecting the number of segments and other complexity-related parameters. As the HSR has multiple control notches, the actual HST operation will be significantly impacted under different traction/braking characteristics according to specific notch. In this case, all notches should be considered in the process of constructing the optimisation model of train speed trajectory in order to reflect the actual operation characteristics more accurately. In this section, we introduced a series of binary variables to represent the corresponding notches to realise the notch selection on the basis of EETC problem of HST.

Energy-efficient train control (EETC) model

As shown in Figure 3, each equidistant segment contains the information about speed change v_i, elapsed time Δt_i and consumed energy E_i, etc. When the train runs from Station A to Station B with a specific applied force F_i, it will encounter speed limits $V_{lim,i}$, resistance f_i and gradient ΔH_i. Further constraint details related to the above variables are formulated as follows.

The entire operation process is discretised into N equidistant segments with length of Δd, which can be expressed by

$$D = \sum_{i=1}^{N} \Delta d \tag{1}$$

where D represents the distance between two adjacent stations and i indicates the index of discrete segments.

Speed limits are imposed to the railway due to the limitation of technical specifications of the train and line requirements. Hence,

$$0 \leq v_i \leq V_{lim,i} \tag{2}$$

needs to be satisfied where $V_{lim,i}$ is the upper limit of train speed at each discrete segment boundary v_i, which depends on the train position.

The energy consumed by HST is mainly used to overcome the drag force caused by mechanical and air friction. We use Davis Equation

$$f_i = A + Bv_{ave,i} + Cv_{ave,i}^2 \tag{3}$$

to calculate the drag force f_i where A, B, C are the Davis coefficients, and $v_{ave,i}$ stands for the average speed of each segment, which can be calculated by

$$v_{ave,i} = \frac{v_i + v_{i-1}}{2}. \tag{4}$$

The journey time is constrained by the timetable, and thus the sum of the elapsed time Δt_i in each

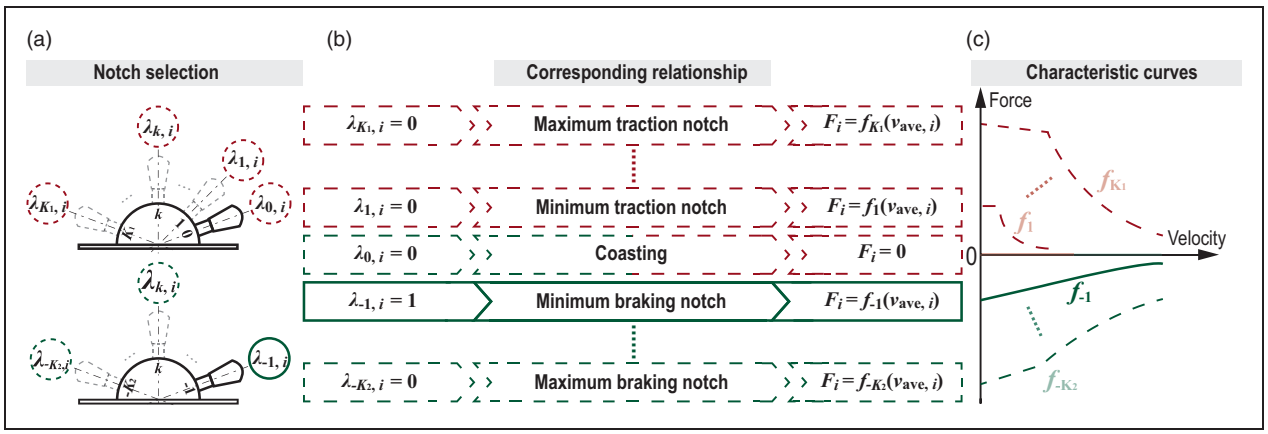

Figure 4. The diagram of the relationship between notches and characteristic curves. (a) Schematics of notch selection. (b) Each binary variable denoted by $\lambda_{k,i}$ corresponds to a traction/braking characteristic function. (c) Visualisation of traction/braking characteristic curves f_k. This figure illustrates the selection of Notch B1 (shown as solid lines) with the binary variable $\lambda_{-1,i}$ to be 1 while others (shown as dashed lines) remain as 0, and the braking characteristic curve f_{-1} is applied to the model.

segment should not exceed the given total time T_{total}. The punctuality constraint is satisfied by:

$$\sum_{i=1}^{N} \Delta t_i = \sum_{i=1}^{N} \frac{\Delta d}{v_{\text{ave},i}} \leq T_{\text{total}} \tag{5}$$

According to the principle of conservation of energy, the relationship among traction/regenerative energy, kinetic energy and potential energy of train, and heat is demonstrated by

$$F_i \Delta d - f_i \Delta d - \frac{1}{2} M (v_i^2 - v_{i-1}^2)$$

$$- Mg \Delta H_i = 0 \tag{6}$$

where F_i represents the applied force obtained from the traction/braking systems according to various notches, M is the total mass of the train, g is the gravitational acceleration and ΔH_i is referred to as the change in height from the previous location to the next as shown in Figure 3.

Equation (7) ensures the acceleration/deceleration would not exceed the maximum value $A_{max,a}$ and $A_{max,d}$:

$$-A_{max,d} \leq \frac{v_{i+1}^2 - v_i^2}{2\Delta d} \leq A_{max,a}. \tag{7}$$

During the entire journey, the electric energy involved in each segment is E_i which could be calculated by

$$E_i \geq F_i \Delta d / \eta_t \tag{8}$$

$$E_i \geq F_i \Delta d \eta_b. \tag{9}$$

where η_t is the traction energy efficiency when $E_i \geq 0$ and η_b is the regenerative energy efficiency when $E_i < 0$.

Thus, the net energy consumption of the whole journey can be demonstrated by:

$$E_{total} = \sum_{i=1}^{N} E_i. \tag{10}$$

Dynamic notch selection model

The notch-control mechanism of HST is designed to offer drivers or ATO selections of different levels of power output from the traction/braking system. As we can see from Figure 2, when HST is operated at a specific speed, different choices of notches will lead to different power output. Moreover, when a certain notch is selected, the applied force of HST would also change along with speed. Accordingly, the speed trajectory of HST will be constantly affected by the dynamic traction/braking characteristics.

It is worth mentioning that some notches could provide equal forces at the same speed. For instance, five different traction efforts are available at 100 km/h, where the largest one can be provided by Notch T5 ~T10 while others are provided by Notch T1 ~T4 separately, as can be seen from Figure 2(a). In this paper, we did not introduce rules to distinguish the notches which determine equal force at the same speed.

Here, a dynamic traction/braking characteristics selection model was constructed by introducing a series of binary variables $\lambda_{k,i}$ to represent the corresponding notches. The correspondence between notches and characteristic curves is illustrated in Figure 4. Once a notch is determined, one of the binary variables is set to be 1. As a result, the traction system of HST would update the specific characteristic curve to regulate the applied force.

To ensure that only one notch is selected at a time, equation (11) needs to be satisfied.

$$\sum_{k=-K_2}^{K_1} \lambda_{k,i} = 1, i = 1, 2, \ldots, N \tag{11}$$

where k is the index of all the notches (including coasting with $k = 0$), K_1 is referred to as the number of traction notches and K_2 represents the number of braking notches. It can be found that the number of binary variables is determined by the model granularity N and the number of notches $(K_1 + K_2 + 1)$.

The applied force of each segment can be calculated by specific characteristic curve according to the corresponding average speed:

$$F_i = \sum_{k=-K_2}^{K_1} \lambda_{k,i} f_k(v_{ave,i}) \tag{12}$$

where f_k demonstrates the characteristic function of k^{th} notch.

Model solution

According to the optimal control theory, the optimal train control strategies involve full traction and full braking. In the proposed discrete model, only selecting the value on the traction/braking characteristic curves as the controlled variable will lead to solution infeasibility due to constraints of the constrained search space. Consequently, it is necessary to relax the constraint of applied force appropriately to guarantee solution feasibility. Moreover, piecewise linearisation is proposed to reduce the difficulty of the problem and improve calculation efficiency.

Vertical relaxation of the applied force

A vertical relaxation was introduced for the applied force in this subsection to deal with the solution infeasibility caused by the strict limitation on the finite discrete notches. In order to demonstrate the necessity of the relaxation more explicitly, take three segments $(N = 3)$ as an example to illustrate this phenomenon firstly.

According to the scenarios of departure and arrival, the first segment must be traction and the last segment should be braking, implying that the speed trajectories are fixed owing to the specific traction/braking forces in the Segment 1 and 3, as shown in Figure 5. In Segment 1, four possible trajectories were produced by Notch T1, Notch T2, Notch T3, and Notch T4 ~T10, in which Notch T4 ~T10 provide the equal force causing the same trajectory with the maximum average speed. When conducting braking, seven different trajectories are generated according to various braking characteristics. To realise the feasibility of the whole journey, trajectory in the Segment 2 has to connect the end point of the first trajectory and the beginning point of the last trajectory. We list all the possibilities of trajectories of Segment 2 with respect to the end point of the first trajectory under all the potential notch restrictions, as shown in Figure 5. The Distance-Speed graphs illustrate the candidate trajectories calculated by the finite discrete notches, and the Speed-Force graphs present the corresponding force with respect to the trajectories in each segment. As can be seen from Figure 5, each final speed of Segment 2 is not equal to the initial speed of Segment 3, i.e. the whole speed curve cannot be connected by the generated candidate trajectories. The infeasibility is caused by the narrow solution space which determined by the finite notches and the discrete model. Accordingly, eliminating this finiteness can make the discrete model solvable.

Given the above illustration, a vertical relaxation method was proposed to relax the constraints of the applied force vertically to guarantee solution feasibility, i.e. to enable the applied force to be available between characteristic curves determined by two adjacent notches. Figure 2(b) reveals the vertical relaxation mechanism for the applied force while choosing Notch B7, and equation (12) can be modified as follows:

$$F_{max,i} = \sum_{k=-K_2}^{K_1} \lambda_{k,i} f_k(v_{ave,i}) \tag{13}$$

$$F_{min,i} = \sum_{k=-K_2}^{K_1} \lambda_{k,i} [f_{k-1}(v_{ave,i}) + (f_k(v_{ave,i}) - f_{k-1}(v_{ave,i}))(1 - P_{con})] \tag{14}$$

$$\begin{cases} F_{min,i} \le F_i \le F_{max,i} & k \ge 0 \\ F_{min,i} \le -F_i \le F_{max,i} & k < 0 \end{cases} \tag{15}$$

where $F_{max,i}$ is referred to as the maximum force which can be applied by the traction system according to the selected notch. $F_{min,i}$ is the minimum force determined by the smaller notch and a control factor P_{con} which represents the possible force range between two adjacent notches. Here, P_{con} ranges from 0 to 100%, but not strictly equal to 0 and 100%. When $P_{con} = 0$, vertical relaxation is not considered which still leads to infeasibility. When $P_{con} = 100\%$, the applied force can be taken both from the two adjacent traction/braking characteristics, which is inconsistent with the uniqueness of notch selection at a certain time. For this reason, a value that closes to 100% can be used to approximate 100% in the cases that applying maximum relaxation.

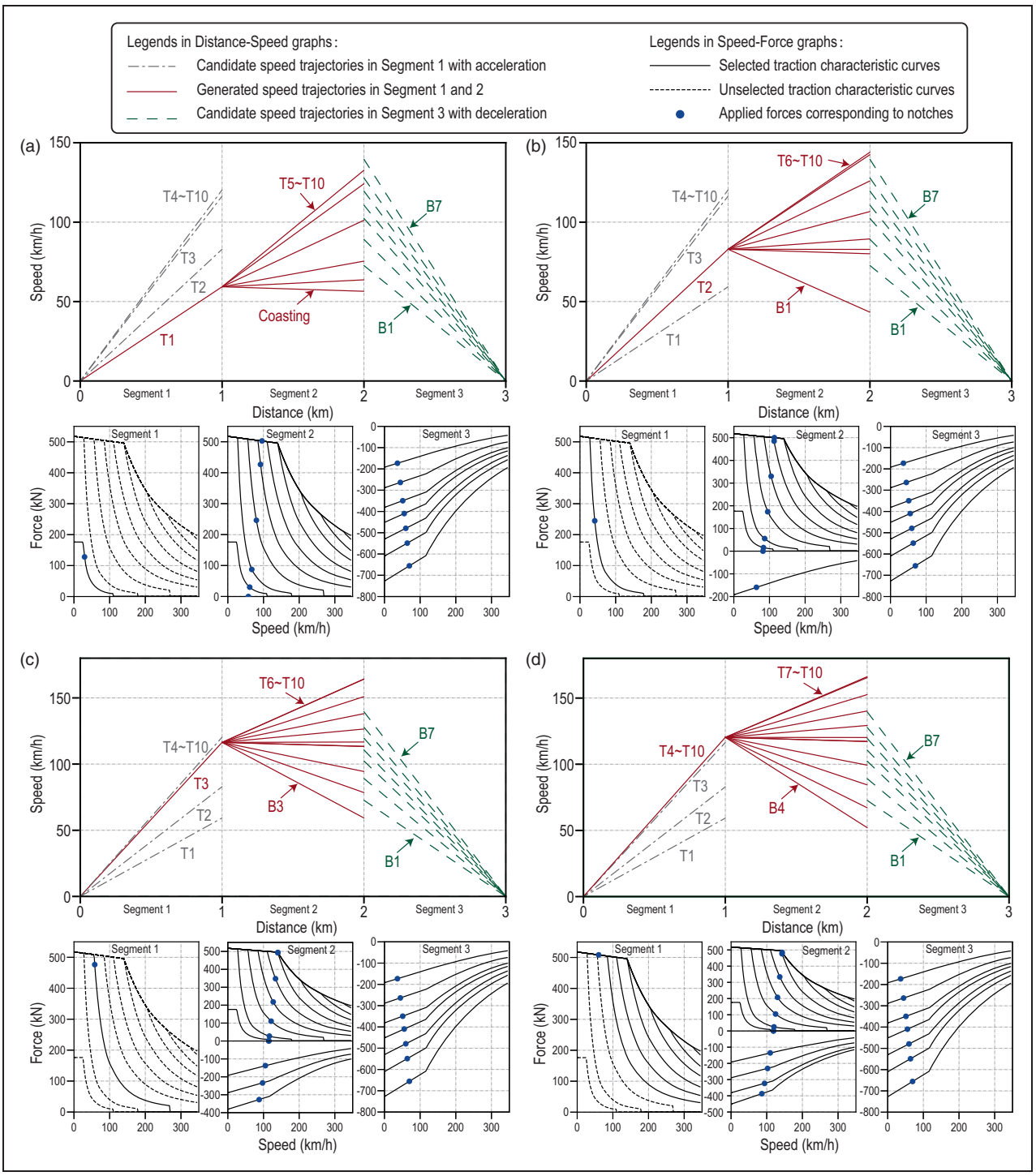

Figure 5. Speed trajectories and the applied force based on the finite discrete notches. Distance-Speed graphs list all the candidate speed trajectories according to the traction/braking characteristics, and the Speed-Force graphs visualise the applied forces on the traction/braking characteristic curves with respect to various speed trajectories. (a)∼(d) illustrates all the possibilities of Segment 2 when Notch T1, Notch T2, Notch T3, and Notch T4 ∼T10 are applied in the Segment 1 respectively. Disconnections of speed between Segment 2 and 3 indicates infeasibility of the solution.

Piecewise linearisation

PWL is an effective method to approximately simplify the complex non-linear variables, which is of great help to the model simplification and calculation while maintaining good precision. The above non-linear variables such as v_i^2, $1/v_{ave,i}$, $v_{ave,i}^2$ and $f_k(v_{ave,i})$ were linearised by PWL, so that the constraints of the MILP model are linear. In order to describe the linearisation in a mathematical way, a special ordered set type 2 (SOS2) is proposed to deal with the variables.[25] In SOS2, at most two variables can be nonzero and these two variables have to be adjacent.

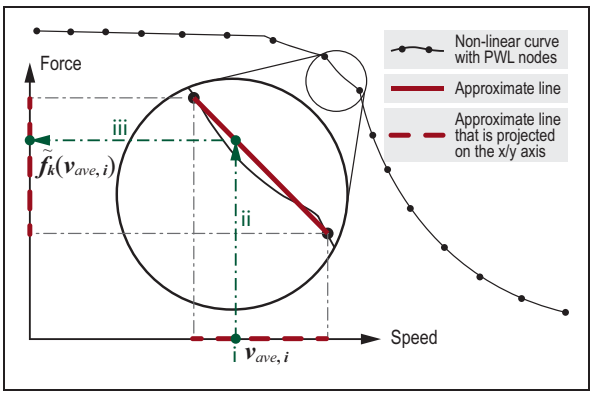

Figure 6. Schematic diagram of linearisation for the non-linear traction/braking characteristic curves $f_k(v_{ave,i})$. i. Find the position of $v_{ave,i}$ on the approximate line that is projected on the x-axis. ii. Generate two adjacent SOS2 variables according to the properties of SOS2 and the position of $v_{ave,i}$. iii. Calculate $\tilde{f}_k(v_{ave,i})$ by the value of SOS2 and the PWL nodes.

Assume that the speed of HST ranges from V_{min} to V_{max}, then a constant δ representing the precision of PWL can be calculated by

$$\delta = (V_{max} - V_{min}/(J-1)) \tag{16}$$

where J is the number of SOS2 variables, which is also the number of PWL nodes.

Taking the linearisation of $f_k(v_{ave,i})$ as an example, the PWL nodes can be added to the model as static parameters in advance. As shown in Figure 6, it is an indirect dynamic affine to determine $f_k(v_{ave,i})$ by $v_{ave,i}$:

(i) The position of $v_{ave,i}$ on the direction of x-axis can be represented by

$$v_{ave,i} = \sum_{j=1}^{J}(V_{min} + (j-1)\delta)\alpha_{i,j}. \tag{17}$$

(ii) SOS2 variables have the following properties:

$$0 \leq \alpha_{i,j} \leq 1, j = 1, 2, \ldots, J \tag{18}$$

$$1 = \sum_{j=1}^{J}\alpha_{i,j}. \tag{19}$$

(iii) Calculate $\tilde{f}_k(v_{ave,i})$ according to the generated SOS2 variables and PWL nodes:

$$\tilde{f}_k(v_{ave,i}) = \sum_{j=1}^{J} F_{point,j}\alpha_{i,j} \tag{20}$$

where $\tilde{f}_k$ is referred to as the approximation of f_k and $F_{point,j}$ are the PWL nodes.

Through the implementation of the above algorithm, the corresponding force can be obtained dynamically along with the changing speed.

The linearisation of $1/v_{ave,i}$, $v^2_{ave,i}$ are shown as follow:

$$1/\tilde{v}_{ave,i} = \sum_{j=1}^{J}\frac{\alpha_{i,j}}{V_{min} + (j-1)\delta} \tag{21}$$

$$\tilde{v}^2_{ave,i} = \sum_{j=1}^{J}(V_{min} + (j-1)\delta)^2\alpha_{i,j} \tag{22}$$

where $1/\tilde{v}_{ave,i}$, $\tilde{v}^2_{ave,i}$ are the approximation of $1/v_{ave,i}$, $v^2_{ave,i}$ respectively.

Another SOS2 $\beta_{i,j}$ was introduced to describe v_i^2:

$$0 \leq \beta_{i,j} \leq 1, j = 1, 2, \ldots, J \tag{23}$$

$$1 = \sum_{j=1}^{J}\beta_{i,j} \tag{24}$$

$$v_i = \sum_{j=1}^{J}(V_{min} + (j-1)\delta)\beta_{i,j} \tag{25}$$

$$\tilde{v}_i^2 = \sum_{j=1}^{J}(V_{min} + (j-1)\delta)^2\beta_{i,j} \tag{26}$$

where $\tilde{v}_i^2$ is the approximation of v_i^2.

Results and discussion

In this section, simulation experiments were carried out based on the computer configuration with *2.5 GHz Intel i7 CPU* and *12 GB RAM*. Many mature commercial optimisers for mathematical programming, e.g. *GUROBI*, *CPLEX*, *LINGO*, etc. can be used to solve the proposed MILP problem. In this paper, *GUROBI 9.0.1* was applied to solve the model subjected to equations (1) to (26) with an objective of minimising E_{total} which is defined by equation (10).

In Case study 1, optimisation results were illustrated to demonstrate the dynamic change of the notch selection with constant speed limit and gradient, showing the feasibility of the proposed notch-based model. Case study 2 was carried out to demonstrate the robustness and effectiveness of the proposed method on the Wuhan-Guangzhou line, which reflects the difference between two MILP models when dealing with a practical line. One of the MILP models is non-notch based which does not consider notch information as the previous work[26–29] did, and treats the traction force as a continuous variable.

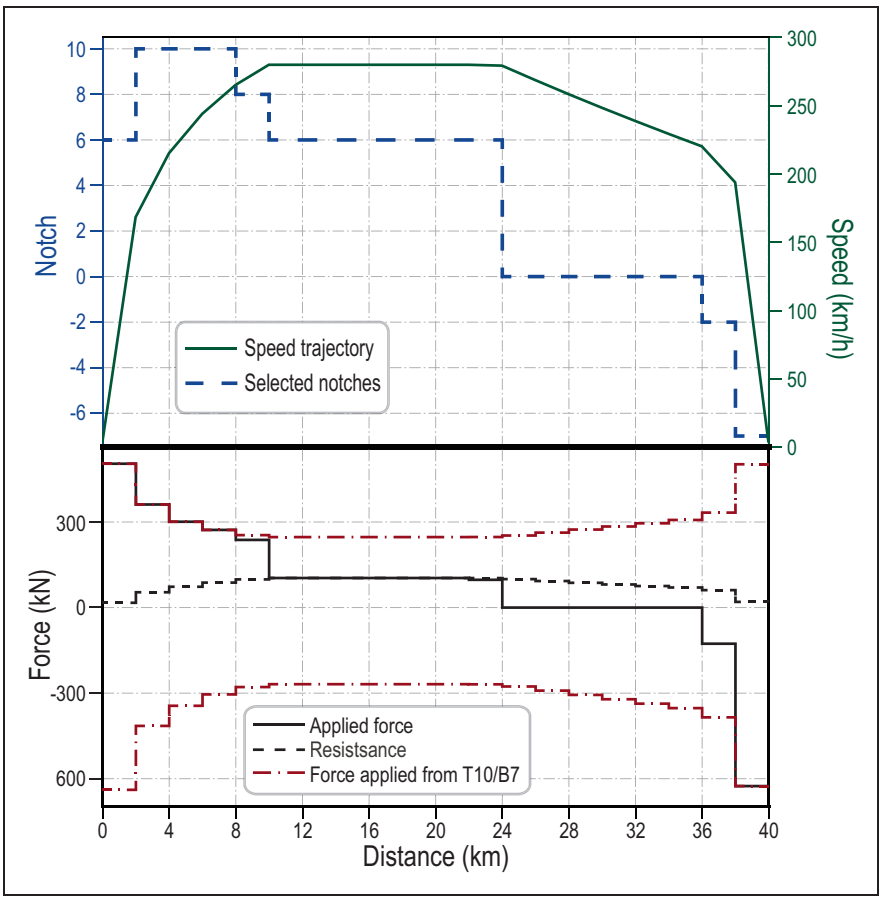

Figure 7. Speed trajectory and selected notches and the corresponding applied force in Case study 1. The applied force demonstrated in the subgraph below changes along with the selected notches and affects the speed trajectory of the train. When the solid line representing the applied force overlaps with the dashed line that represents the resistance, the train conducts a cruising operation, otherwise, it would lead to acceleration or deceleration.

The other MILP model is notch-based proposed in this paper which considers muti-notch characteristics to study notch strategy and its impact on the train operation.

All the cases adopt the data of China CRH380AL HST. The modelling parameters are shown in Table 1, and the traction/braking characteristics are obtained from Figure 2.

Case study 1: feasibility validation of the model on an artificial line

In this subsection, an artificial line was adopted to demonstrate the dynamic notch selection and the changing applied force under the specific restriction from various notch characteristics. In order to eliminate the influence of other factors, constant speed limit and gradient were adopted here. In this case study, P_{con} equals 99%, to approximate 100% to realise a maximum relaxation.

The optimal speed trajectory and selected notches with corresponding force information are illustrated in Figure 7, where the upper subgraph visualises the speed trajectory and selected notches and the subgraph below illustrates the actual applied force and the resistance that HST encounters. The maximum force of the traction/braking system (determined by Notch T10 and Notch B7) is also displayed to

Table 1. Modelling parameters for Case study 1 & Case study 2.

	Value	
Parameter	Case study 1	Case study 2
D(km)	40	48
T_{total}(s)	670	1000
V_{lim}(km/h)	280	(in Figure 9)
N	20	48
J	31	20
P_{con}(%)	99	99
M(t)	890	
K_1	10	
K_2	7	
$A_{max,a}$(m/s^2)	1.2	
$A_{max,d}$(m/s^2)	1.2	
η_t	0.9	
η_b	0.6	
A(kN)	5.2	
B(kN/(km/h))	0.038	
C(kN/(km^2/h^2))	0.00112	

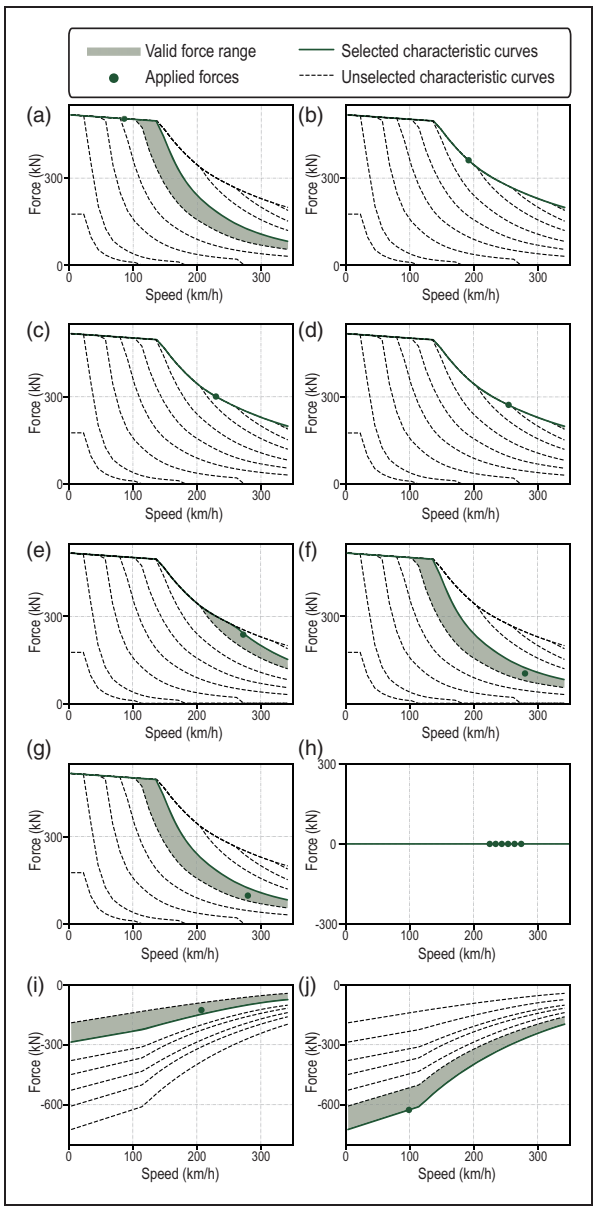

Figure 8. Dynamic notch selection and the applied force in Segment 1∼20 of Case study 1. The dashed lines indicate the unselected traction/braking characteristic curves. The solid lines represent the selected traction/braking characteristic curves. The shaded parts visualise the valid range of the applied force changing along with the notch selection. The dots represent the actual force applied in each segment.

indicate the validity of the applied force. Figure 8 reveals the dynamic notch selection with different notch characteristics applied in the model in each segment.

As can be seen from Figure 7, the train conducts traction during Segment 1 ∼5 where the traction force is greater than the resistance with selections of the Notch T6, Notch T10, and Notch T8. Due to the changing speed and varying notch, the applied force varies along the traction characteristic curves and maintains a full traction in the first four segments shown in Figure 8(a) to (d). The applied forces are obtained from the characteristic curves, indicating that vertical relaxation is not adopted. Since no corresponding rules are introduced to distinct the equal forces offered by various notches, there is no difference in the selection of Notch T6 ∼T10 for the first four segments. It is noted that the train applies a traction force which is between the traction characteristic curves of Notch T7 and T8 according the vertical relaxation rule, which implies a partial traction, as shown in Figure 8(e). During the cruising phase of Segment 6 ∼11, the applied traction force is equal to the resistance. In the practical situation, the resistance of the train would not always be equal to a value on the traction characteristic curves at a specific speed. In order to perfectly counteract the resistance and carry out cruising, the above-mentioned vertical relaxation is needed to applied. As shown in Figure 8 (f), the traction force satisfying the condition of cruising is located between Notch T5 and Notch T6. During Segment 12, a smaller traction force is applied which leads to a slight deceleration that belongs to the state between cruising and coasting as shown in Figure 8(g). In the deceleration stage, the train coasts during Segment 13 ∼18 with no power supplied, and then conducts partial braking in the Segment 19 and a full braking in the Segment 20, as shown in Figure 8(h) to (j).

Based on the above analysis, the optimal speed trajectory not only contains the full traction, cruising, coasting, and full braking which are the classical regimes derived by the optimal control theory, but also performs partial traction and partial braking that connects the classical regimes to each other. By adopting the vertical relaxation, partial traction/braking can be realised to achieve a feasible solution with finite notches.

Case study 2: robustness and effectiveness validation with a practical line

In reality, HSTs are faced with changing or temporary speed limits and varying gradient. A case in a real-world scenario is investigated in this subsection with a simulation of the multi-notch concerned in this paper and a non-notch simulation that is conducted in the previous papers. The route information comes from a section of Wuhan-Guangzhou line and the parameters can easily adapt to simulate other real-word cases. The speed trajectory and notch selection strategy in the multi-notch simulation with the constraints of changing speed limit and varying gradient are illustrated in Figure 9(a). Figure 9(b) depicts the non-notch based situation with the same route condition as used in simulation with multi-notch characteristics.

It can be found that the speed trajectory in the multi-notch simulation is similar to that of non-notch situation. Due to the characteristics of notch control, a small fluctuation occurs near 300 km/h as illustrated in the speed trajectory in Figure 9(a),

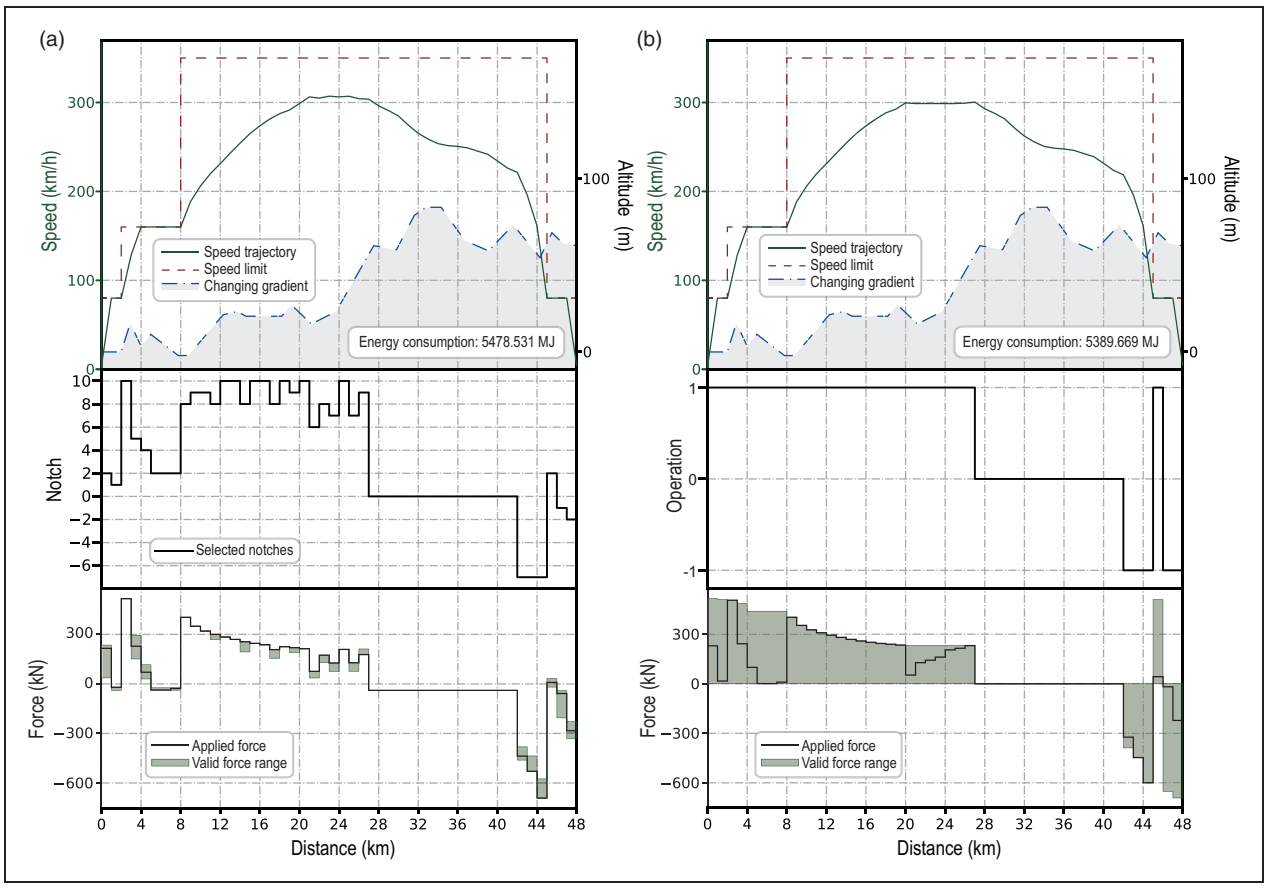

Figure 9. Speed trajectory and selected notches and the corresponding applied force in the real-word case. (a) it illustrates the optimal result of the proposed multi-notch model. By selecting various notches and applying maximum vertical relaxation, the applied forces are obtained from the valid range as shown by the shaded area. (b) it visualises the optimal result without multi-notch information. "1" represents traction operation, "0" indicates coasting operation, and "-1" means braking operation. Since the applied force is a continuous variable, it can be taken from 0 to the maximum value as the shaded area has shown.

which may lead to a rise in energy consumption compared to the non-notch situation. Nonetheless, a more practical speed trajectory is obtained by introducing the multi-notch characteristics compared with non-notch situation and the total energy consumption of model considering multiple notches is increased by 1.622% from 5389.669 MJ to 5478.531 MJ. The optimal results indicate that the model maintains robustness when dealing with changing speed limits and varying gradient. Moreover, some segments adopt vertical relaxation to ensure the feasibility of the solution, while others keep restriction on the characteristic curves with dynamic notches.

Conclusion and future work

In this paper, a notch-based mixed integer linear programming (MILP) model is proposed, which could adjust the applied force dynamically under the constraint of static notch information and obtain both energy-efficient speed trajectory and notch selection strategy. Different from the other studies that regard the applied force as a continuous variable, this paper introduces a series of binary variables to model specific notches based on the fact that the high-speed train (HST) is equipped with multiple notches. In order to provide a sufficient solution space for the discrete model, the vertical relaxation technique is adopted to allow the applied force to be selected between two adjacent traction/braking characteristic curves according to a control factor P_{con}. Piecewise linearisation (PWL) is utilised to approximately linearise the complex non-linear variables, which is of great effectiveness to model simplification and calculation while maintaining a high degree of precision. Case study 1 indicates that the model is effective to achieve notch selection and adjust the applied force dynamically with respect to the changing speed. In Case study 2, variable speed limit and gradient are considered whose data comes from CRH380AL HST and the subline of Wuhan-Guangzhou HSR, showing effectiveness and robustness of the proposed model. In conclusion, the model proposed in this paper could obtain a more practical speed trajectory considering multi-notch characteristics. The notch-based model is able to obtain a more realistic optimal strategy containing dynamic notch selection and speed trajectory with an increase (1.622%) in energy consumption by comparing the results of the proposed model and the non-notch model.

In terms of future work, the proposed model will be further expanded to solve the speed trajectory optimisation problem with multi-notch and multi-mass characteristics for HSR and heavy-hauled trains.

Acknowledgements

This paper is an extension to our previously published conference paper *A New Operation-Oriented Mixed Integer Linear Programming Model for Energy-Efficient Train Operations* on 2020 10th International Conference on Power and Energy Systems (ICPES), 350-355.

Declaration of Conflicting Interests

The author(s) declared no potential conflicts of interest with respect to the research, authorship, and/or publication of this article.

Funding

The author(s) disclosed receipt of the following financial support for the research, authorship, and/or publication of this article: The work described in this paper has received funding from the State Key Laboratory of Rail Traffic Control and Safety(Contract No.RCS2021K008), Beijing Jiaotong University, and in part by the Fundamental Research Funds for the Central Universities NO. 2020ZYGXZR087.

ORCID iD

Shaofeng Lu https://orcid.org/0000-0001-5361-2463

References

1. Watanabe S, Koseki T and Isobe E. Evaluation of automatic train operation design for energy saving based on the measured efficiency of a linear-motor train. *Electr Eng Jpn* 2018; 202: 50–61.
2. Zhang Y, Chen Z, Wang J, et al. Research on the comfort control technology of the ATO system in high-speed railway. *J Railw Eng Soc* 2019; 36: 67–71.
3. Yin J, Tang T, Yang L, et al. Research and development of automatic train operation for railway transportation systems: a survey. *Transport Res C* 2017; 85: 548–572.
4. ShangGuan W, Yan X, Cai B, et al. Multiobjective optimization for train speed trajectory in CTCS high-speed railway with hybrid evolutionary algorithm. *IEEE Trans Intell Transport Syst* 2015; 16: 2215–2225.
5. Ichikawa K. Application of optimization theory for bounded state variable problems to the operation of train. *Bull JSME* 1968; 11: 857–865.
6. Howlett P. The optimal control of a train. *Ann Oper Res* 2000; 98: 65–87.
7. Khmelnitsky E. On an optimal control problem of train operation. *IEEE Trans Automat Contr* 2000; 45: 1257–1266.
8. Albrecht A, Howlett P, Pudney P, et al. The key principles of optimal train control-part 1: formulation of the model, strategies of optimal type, evolutionary lines, location of optimal switching points. *Transport Res B: Methodological* 2016; 94: 482–508.
9. Lai Q, Liu J, Haghani A, et al. Energy-efficient speed profile optimization for medium-speed maglev trains. *Transport Res E* 2020; 141: 102007.
10. Goverde RM, Scheepmaker GM and Wang P. Pseudospectral optimal train control. *Eur J Oper Res* 2020; 292: 353–375. DOI:10.1016/j.ejor.2020.10.018.
11. Trivella A, Wang P and Corman F. The impact of wind on energy-efficient train control. *EURO J Transport Logist* 2020; 10: 1–29. DOI: 10–1016. /j. ejtl.2020.100013.
12. Zhao Y and Zhang P. Research and prospect of automatic train operation technology for high-speed railway. *Railw Signal Commun* 2019; 55: 75–80.
13. Dong H, Ning B, Cai B, et al. Automatic train control system development and simulation for high-speed railways. *IEEE Circuits Syst Mag* 2010; 10: 6–18.
14. Zhou L, Tong L(C), Chen J, et al. Joint optimization of high-speed train timetables and speed profiles: a unified modeling approach using space-time-speed grid networks. *Transport Res B: Methodological* 2017; 97: 157–181.
15. Zhong W, Li S and Xu H. On-line train speed profile generation of high-speed railway with energy-saving: a model predictive control method. *IEEE Trans Intell Transport Syst* 2020; 1–12. DOI: 10–1109. /TITS.2020.3040730.
16. He D, Zhou L and Sun Z. Energy-efficient receding horizon trajectory planning of high-speed trains using real-time traffic information. *Control Theor Technol* 2020; 18: 204–216.
17. Yan XH, Cai BG, Ning B, et al. Moving horizon optimization of dynamic trajectory planning for high-speed train operation. *IEEE Trans Intell Transport Syst* 2016; 17: 1258–1270.
18. Peng J. *Traction and braking of EMU*. Beijing: China Railway Publishing House, 2009.
19. Zhang L and Zhuan X. Optimal operation of heavy-haul trains equipped with electronically controlled pneumatic brake systems using model predictive control methodology. *IEEE Trans Contr Syst Technol* 2014; 22: 13–22.
20. Tang H, Wang Y, Liu X, et al. Reinforcement learning approach for optimal control of multiple electric locomotives in a heavy-haul freight train: a double-switch-Q-network architecture. *Knowledge-Based Syst* 2020; 190: 105173.
21. Li YZ, Wang Pl, Lin X, et al. High-speed automatic train operation optimization algorithm. *J Comput Appl* 2012; 32: 3221–3224.
22. Yang H and Zhang YJ. K. Multiple-model self-tuning fuzzy PID control of braking process of electric multiple unit. *J China Railw Soc* 2014; 36: 42–47.
23. Li Y and Hou Z. Study on energy-saving control for train based on genetic algorithm. *J Syst Simul* 2007; 19: 384–387.
24. Zhang J and Wu X. Study on target speed profile of high-speed train ATO under temporary speed restriction conditions. *Railw Standard Des* 2020; 64: 168–174.
25. Bisschop J. Linear programming tricks. In: AIMMS (ed.) *AIMMS optimization modeling*. AIMMS B.V., 2021, pp. 62–74.
26. Wang Y, De Schutter B, van den Boom TJ, et al. Optimal trajectory planning for trains - a pseudospectral method and a mixed integer linear programming

approach. *Transport Res C: Emerging Technol* 2013; 29: 97–114.
27. Lu S, Wang MQ, Weston P, et al. Partial train speed trajectory optimization using mixed-integer linear programming. *IEEE Trans Intell Transport Syst* 2016; 17: 2911–2920.
28. Tan Z, Lu S, Bao K, et al. Adaptive partial train speed trajectory optimization. *Energies* 2018; 111–133.
29. Wu C, Zhang W, Lu S, et al. Train speed trajectory optimization with on-board energy storage device. *IEEE Trans Intell Transport Syst* 2019; 20: 4092–4102.

Appendix

Notation

Parameters

A	Davis coefficient [kN].
$A_{max,a}$	maximum acceleration [m/s^2].
$A_{max,d}$	maximum deceleration [m/s^2].
B	Davis coefficient [k$N/(m/s)$].
C	Davis coefficient [k$N/(m^2/s^2)$)].
D	distance between two adjacent stations [m].
g	gravitational acceleration [m/s^2].
J	total number of piecewise linearisation nodes.
K_1	total number of traction notches.
K_2	total number of braking notches.
M	mass of the high-speed train [kg].
N	total number of discrete segments.
P_{con}	control factor in the vertical relaxation [%].
T_{total}	preset travel time between two adjacent stations [s].
$V_{lim,i}$	preset speed limit at every discrete point [m/s].
V_{max}	maximum speed of the train [m/s].
V_{min}	minimum speed of the train [m/s].
δ	precision of piecewise linearisation.
Δd	distance of every discrete segment [m].
ΔH_i	gradient change in every discrete segment [m].
ηb	regenerative braking energy efficiency.
ηt	traction energy efficiency.

Variables

E_i	energy consumption in every discrete segment [J].
E_{total}	net energy consumption of the whole journey [J].
F_i	applied force in every discrete segment [N].
f_i	average drag force in every discrete segment [N].
f_k	characteristic function of kth notch [N].
$F_{max,i}$	maximum traction/braking force in every discrete segment [N].
$F_{min,i}$	minimum traction/braking force in every discrete segment [N].
i	index of ith discrete segment.
j	index of piecewise linearisation nodes.
k	index of notches.
v_i	train speed at every discrete point [..].
$v_{ave,i}$	average speed in every discrete segment [m/s].
$\alpha_{i,j}$	SOS2 variables for speed-related variables linearisation.
$\beta_{i,j}$	SOS2 variables for average-speed-related variables linearisation.
Δt_i	elapsed time in every discrete segment [..].
$\lambda_{k,i}$	binary variables to represent the corresponding notches.

Abbreviations

ATO	automatic train operation
EETC	energy-efficient train control
GA	genetic algorithm
HSR	high-speed railway
HST	high-speed train
MILP	mixed integer linear programming
MPC	model predictive control
MTTC	minimum-time train control
PMP	Pontryagin's maximum principle
PWL	piecewise linearisation